

This article was downloaded by:

On: 26 January 2011

Access details: *Access Details: Free Access*

Publisher *Taylor & Francis*

Informa Ltd Registered in England and Wales Registered Number: 1072954 Registered office: Mortimer House, 37-41 Mortimer Street, London W1T 3JH, UK



Liquid Crystals

Publication details, including instructions for authors and subscription information:

<http://www.informaworld.com/smpp/title~content=t713926090>

Optical properties of stretched polymer dispersed liquid crystal films

O. A. Aphonin^a; Yu. V. Panina^a; A. B. Pravdin^a; D. A. Yakovlev^a

^a Department of Physics, University of Saratov, Saratov, Russia

To cite this Article Aphonin, O. A. , Panina, Yu. V. , Pravdin, A. B. and Yakovlev, D. A.(1993) 'Optical properties of stretched polymer dispersed liquid crystal films', *Liquid Crystals*, 15: 3, 395 – 407

To link to this Article: DOI: 10.1080/02678299308029140

URL: <http://dx.doi.org/10.1080/02678299308029140>

PLEASE SCROLL DOWN FOR ARTICLE

Full terms and conditions of use: <http://www.informaworld.com/terms-and-conditions-of-access.pdf>

This article may be used for research, teaching and private study purposes. Any substantial or systematic reproduction, re-distribution, re-selling, loan or sub-licensing, systematic supply or distribution in any form to anyone is expressly forbidden.

The publisher does not give any warranty express or implied or make any representation that the contents will be complete or accurate or up to date. The accuracy of any instructions, formulae and drug doses should be independently verified with primary sources. The publisher shall not be liable for any loss, actions, claims, proceedings, demand or costs or damages whatsoever or howsoever caused arising directly or indirectly in connection with or arising out of the use of this material.

Optical properties of stretched polymer dispersed liquid crystal films†

by O. A. APHONIN*, YU. V. PANINA, A. B. PRAVDIN
and D. A. YAKOVLEV

Department of Physics, University of Saratov,
Astzakhanskaya 83, 410071 Saratov, Russia

(Received 11 December 1992; accepted 16 March 1993)

The basic mechanisms determining the formation of optical anisotropy in stretched, thin polymer dispersed liquid crystal (PDLC) films with micron sized nematic droplets have been studied experimentally and the results analysed in terms of a proposed theoretical model. The experiments were performed on PDLC films with the bipolar nematic director configuration in the droplets, where the film transmittance, microscopic structure, and birefringence of the polymer matrix were studied. It is shown that the orientational ordering of bipolar nematic droplets, introducing the main contribution to the ability of stretched PDLC film to polarize the transmitted light, is strongly dependent upon initial droplet shape and the elastic properties of the polymer matrix. The 'anomalous' nematic director orientation is also observed in a portion of elongated droplets where the axes of bipolar configurations do not coincide with the major axes of the droplet cavities due to the presence of inclusions at the cavity walls. The effect of alternation of droplet size and shape upon stretching and the influence of optical anisotropy of the polymer matrix on film transmittance are analysed. On the basis of the results obtained, simple criteria for optimization of main PDLC polarizer performance are formulated.

1. Introduction

In recent years, there has been much study of polymer dispersed liquid crystals (PDLC) consisting of liquid crystal (LC) microdroplets, having sizes of the order of microns, embedded in a transparent polymer matrix [1-4]. The interest in these composite materials results from a wide variety of their potential applications in light shutters, displays, switchable windows, and other devices, which are based on electrically or thermally controlled light scattering by PDLC films [5]. PDLC technology also provides the possibility of producing effective electrically controlled non-absorptive polarizers, which are attractive for use with powerful radiation when the conventional film polarizers (polaroids) are unstable (for example, the extinction ratio of PDLC polarizer may be 10^3 or higher, the power of the incident radiation being of the order of kilowatts per cm^2) [6-8]. The operating principle of a PDLC polarizer is based on the effect of anisotropic light scattering by PDLC films with unidirectionally oriented nematic droplets having the so called bipolar director configuration (see figure 2(a) for a schematic representation). If the ordinary refractive index of the nematic is chosen to match closely the refractive index of the polymer matrix, the components of normally incident light in the direction of the droplet ordering will be strongly scattered due to the large mismatch between the refractive index of the polymer matrix and the effective refractive index of the bipolar nematic droplets in this direction. In contrast, the components of incident light in a perpendicular direction will encounter a refractive

* Author for correspondence.

† Presented at the Fourteenth International Liquid Crystal Conference, 21-26 June 1992, University of Pisa, Italy.

index within the droplets that is similar to the polymer matrix index, and will be transmitted through the film unaffected. As a result, the unpolarized incident light will be partially polarized after passing through the oriented PDLC film. If the dielectric anisotropy of the nematic is positive, a scattering PDLC polarizer can be switched to a non-polarizing, light transmissive state by applying an external electric field of sufficient strength normal to the film surface. In this state, the liquid crystal director in all droplets is oriented in a direction parallel to the field, with the result that the refractive index matching occurs for all components of normally incident light, thereby allowing incident light to pass through unpolarized.

The required unidirectional alignment of bipolar droplets in a PDLC polarizer can be produced by several methods including polymerization of the matrix in the presence of a strong longitudinal electric or magnetic field, shearing deformation, or stretching the film [6, 7, 9]. Among these methods, stretching is the most effective, for it provides a high degree of droplet ordering and a good controllability of the ordering process. To be able to optimize the performance of such a polarizer, it is desirable to understand the factors determining the formation of optical anisotropy in a stretched PDLC film. In this paper we report an experimental and theoretical study to explain and quantify the main mechanisms governing the anisotropic transmittance of PDLC films, with particular emphasis on the effects of LC droplet orientation, size and shape. Initially, in §2, we present the results of transmittance measurements for laser light and data from microscopic studies of PDLC films under the stretching. In §3 we propose the theoretical model of the droplet reorientation mechanism in the polymer matrix and analyse the factors determining the optical behaviour of PDLC films during the stretching process. Then, in §4, we test theoretical predictions by comparing them with experimental data and explain some of the observed phenomena in terms of the model proposed. Finally, we formulate, on the basis of the results obtained, simple criteria for optimization of main PDLC polarizer performance.

2. Experimental section

2.1. Samples and experimental procedures

The PDLC films analysed in this paper were prepared by the polymer encapsulation method described in detail by Drzaic [3]. The nematic mixture SZK-1 (similar to BDH E7 LC mixture) was emulsified in an aqueous solution of a polyvinyl alcohol (PVA)/glycerine mixture, with a glycerine content of 10 per cent with reference to pure PVA by weight. Glycerine was used as a plasticizer. The index match resulting from these materials is quite good. The emulsion was then coated on to a clear glass plate by drawing a knife edge with adjustable gap over the plate surface and the film was then dried under ambient conditions. The droplet size distribution in the emulsion, measured by optical microscopy, covered the droplet diameter range from approximately 1 to 7 μm and had an optimum at about 2 μm . The volume fraction of LC droplets in dried films used in our experiments varied from 0.05 to 0.2, and the film thickness lay in the region from 15 to 40 μm . For transmittance measurements and microscopic studies, rectangular specimens 30 \times 20 mm were cut from sheets of dried PDLC film and then placed in a special mechanical unit providing controllable unidirectional stretching of the film. The transmittance measurements were performed on an optical bench system, using well collimated He-Ne laser light (632.8 nm) normal to the film surface and a half-wave plate coupled with a polarizer placed between the laser and the PDLC film. The light transmitted by the PDLC film at its centre was

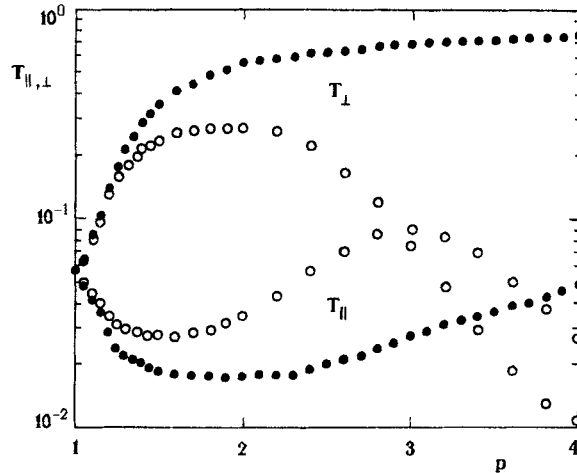


Figure 1. The relative transmittance of a stretched PDLC film as a function of the degree of film extension, p , for the case of normal incidence of light from a He-Ne laser ($\lambda = 633 \text{ nm}$), polarized parallel (T_{\parallel}) and perpendicular (T_{\perp}) to the stretch direction. The film thickness is $20 \mu\text{m}$ and the droplet volume fraction is 0.15. Other film parameters are presented in the text. The open circles represent the data for freely stretched PDLC film. The solid circles represent the data for PDLC film with glycerine immersion coatings. The data are normalized with respect to the transmittance of a pure PVA/glycerine matrix placed (solid circles) or not placed between two glass plates with glycerine immersion.

collected on to a detector within a cone of 0.25° half angle about the axis of the detection system. Two series of transmittance measurements were carried out: when PDLC films were freely stretched, and when they were covered by immersion coatings during the stretching process. In the latter case, before the stretching, a thin film of glycerine, which was used as an immersant, was smeared on to the front and rear surfaces of the PDLC film, and then the whole was laminated between two glass slides. As a result, good quality immersion coatings were formed at both surfaces of the film clamped between the glass slides. This procedure allowed us to eliminate the influence of any surface defects and roughness in the PDLC film on its transmittance. The microscopic structures of the diluted ($10\times$ by weight) PDLC films were studied using polarizing microscopy with a magnification up to $1200\times$. The refractive indices of the polymer matrix on stretching were obtained by precisely measuring Brewster angles with a goniometric unit at a wavelength of 633 nm .

2.2. Results

(i) *Transmittance of stretched PDLC film.* The transmittance of a thin PDLC film as a function of the degree of film extension, p , determined as the ratio of local film length in the deformed and undeformed states, is shown in figure 1 for light polarized parallel (T_{\parallel}) and perpendicular (T_{\perp}) to the stretch direction. As we can see, there is a pronounced difference in the behaviour of the $T_{\parallel}(p)$ and $T_{\perp}(p)$ dependences for films with immersion and without immersion at $p \geq 2$. Detailed study of freely stretched PDLC films showed the existence of numerous surface defects at the film surfaces for large p . These defects cause intensive, predominantly forward, light scattering for both \parallel and \perp polarizations, which strongly alters $T_{\parallel}(p)$ and $T_{\perp}(p)$ dependences. On the contrary, for the PDLC film with immersion coatings, a large extinction ratio, T_{\perp}/T_{\parallel} , is observed for all values of $p \geq 2$ because the effect of surface defects is eliminated. This

fact allowed us, by increasing the initial film thickness and droplet volume fraction up to $35\ \mu\text{m}$ and 0.2 respectively, to produce a PDLC polarizer having a value of the extinction ratio more than 10^3 and a transmittance of the \perp -polarized component higher than 60 per cent at a light wavelength of 632.8 nm.

(ii) *Microscopic studies of PDLC films.* To be able to interpret the macroscopic properties of PDLC films in terms of the processes occurring at the microscopic level, we have performed intensive microscopic studies of diluted PDLC films on stretching. These studies have revealed the following features:

- (a) In undeformed films, the droplet cavities are non-spherical so that their shape in the film plane may be approximated by an ellipse with a small aspect ratio $l \approx 1.2$, the major axes of the ellipse-like cavities being randomly distributed in the plane. The observed distortion of droplet shape seems to be a result of strain arising from the matrix polymerization process during solvent evaporation. This strain also makes the droplets oblate in the film plane, as observed from electron micrographs by other workers [10–12]. Thus, the droplet cavities in unstretched PDLC films seem capable of treatment as general ellipsoids, with their minor axes aligned perpendicular to the film plane, but a random distribution of the major axes of the ellipsoids within the plane. The nematic in the droplets adopts a bipolar configuration which usually occurs under tangential boundary conditions at the polymer walls of the droplet cavity [13]. This configuration is shown schematically in figure 2 (a). The axes of the bipolar configurations (the imaginary straight lines connecting two point defects in the nematic at the droplet surface) in most droplets are therewith aligned along the major axes of the ellipsoidal cavities, and thus, also lie in the film plane.
- (b) Stretching a PDLC film causes the droplet cavities within the film to form prolate ellipsoids aligned with their major axes along the stretch direction, and the bipolar axes inside the cavities are also aligned along this direction (see figure 2 (a)). Further stretching results in further elongation of the droplet cavities and makes them thinner. The film dimensions therewith follow the equation

$$L_x \approx p, \quad L_y \approx p^{-A}, \quad L_z \approx p^{-B}, \quad A + B = 1. \quad (1)$$

Here the coordinate system XYZ has X axis parallel to the stretch direction and the Z axis normal to the film surface. Equation (1) indicates that there was

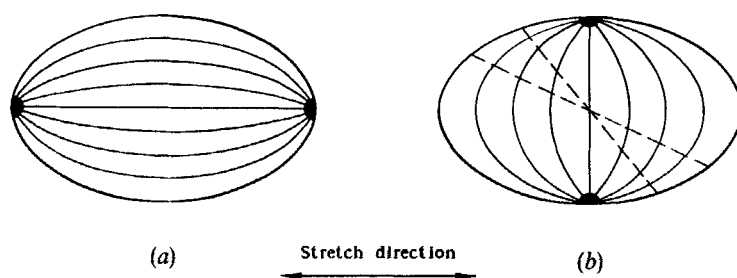


Figure 2. Schematic representation of (a) the typical orientation of the bipolar director configuration in a prolate (ellipsoidal) nematic droplet, and (b) the orientation of the bipolar configuration in an 'anomalous' droplet. The ends of the broken lines represent possible locations of configuration poles at the droplet surface.

no volume change in the film on stretching. Separate experiments have shown that this involves an error of less than 1 per cent. In the centre of the films, where all optical and microscopical measurements were carried out, A and B had the values $A \approx 0.4$ and $B \approx 0.6$. Note that observations (a) and (b) are in a good agreement with previous results published [3, 10–12].

- (c) At the same time, the positions of the bipolar axes in a portion of the droplets do not coincide with the major axis of ellipsoidal cavities. The possible positions of the poles of the bipolar configuration in this case are schematically shown in figure 2(b). The number of these ‘anomalous’ droplets decreases as p increases, and at sufficiently high values of p , all droplets are aligned along the stretch direction. We believe that the reason for this observed phenomenon is probably connected with the presence of surface defects (inclusions) at the droplet walls, which tend to trap the poles of the bipolar nematic configuration. However, this phenomenon requires a detailed study.
- (d) The formation of surface defects was observed in PDLC films with increasing p . These defects are the open cavities on both surfaces of the film and are a result of destruction of large droplets. The number of defects increases as p grows, and for $p > 4$, the film surfaces are densely covered with defects. Since the cavities are large and filled with air, predominantly forward diffraction occurs from them, resulting macroscopically in strong depolarization of light transmitted through the bulk of the PDLC film.

(iii) *Optical properties of the PVA/glycerine matrix.* Studies of the stretched pure PVA/glycerine matrix showed that the matrix itself was clear and defectless over the whole range $1 \leq p \leq 4$, but demonstrated a pronounced birefringence, which increases with film stretching. The results of measuring the principal refractive indices of PVA/glycerine matrix are shown in figure 3. The growth of matrix anisotropy is caused by ordering of the polymer crystallites in the film on stretching and this is described in detail, for example, in [14].

Thus, the main factors determining the optical behaviour of stretched PDLC films, when the adverse effect of surface defects is eliminated, can be summarized as follows:

- (1) the orientational ordering of the LC droplets in the polymer matrix;
- (2) the change of shape and size of LC droplets, producing alterations in their scattering properties;
- (3) the growth of birefringence of the polymer matrix with the growth of deformation.

It is obvious that the cooperative effect of these factors on PDLC film transmittance is quite complicated and needs a detailed theoretical analysis which will be performed in the next section.

3. Theoretical model

3.1. Mechanism of droplet reorientation

The following assumptions are used: (i) The shapes of LC droplets in underformed PDLC film are generally ellipsoidal with axes $a_0 \geq b_0 \geq c_0$. The axes a_0 and b_0 lie in the plane of film and have random orientation. (Note that this assumption agrees well with the results of experimental observations, presented above.) (ii) All droplets are identical in initial shape (aspect ratios $l_0 = a_0/b_0$ and $l_1 = a_0/c_0$ are independent of droplet size). (iii) All droplets have ideally smooth surfaces without any inclusions (‘anomalous’

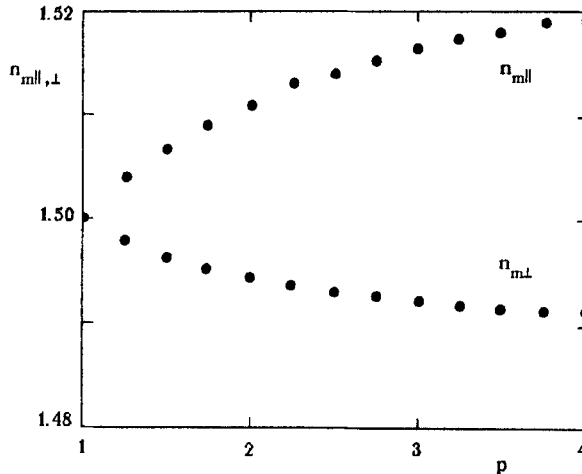


Figure 3. The refractive indices of a stretched PVA/glycerine matrix as a function of the degree of film extension, p , for light polarized parallel ($n_{m||}$) and perpendicular ($n_{m\perp}$) to the stretch direction. The data were obtained by measuring Brewster angles at a wavelength of 633 nm.

droplets are ignored); polymer surface alignment effects are also neglected. In view of the assumptions made, the axes of the bipolar director configurations inside the droplets are presumed to be oriented along the major axes of the ellipsoids, because the nematic elastic energy is minimized in this position [9, 15].

It may be shown from purely geometrical considerations that, with assumptions made and under deformation described by equation (1), the initial ellipsoid with axes a_0 , b_0 , c_0 and the orientation angle α_0 with respect to the stretch direction (see figure 4(a)) tends to transform into the ellipsoid of equal volume having parameters a , b , c and α which are described by the following expressions

$$\frac{a}{b} = \frac{\sqrt{2a_0p}}{\sqrt{[K_2 \mp \sqrt{(K_1^2 + M^2)}]}}}, \quad c = a_0/l_1 p^B, \quad \tan 2\alpha = \frac{M}{K_1}, \quad (2a)$$

where

$$\frac{K_1}{K_2} = [p^{2(A+1)}l_0^2 \mp 1] \cos^2 \alpha_0 \mp [l_0^2 \mp p^{2(A+1)}] \sin^2 \alpha_0, \quad (2b)$$

$$M = (l_0^2 - 1)p^{A+1} \sin 2\alpha_0. \quad (2c)$$

In accordance with equation (2), the transition to the state with an ordered orientation of the system is modeled as a turning of the major axes of the ellipsoids towards the stretch direction, the poles of the bipolar configuration inside the droplets being located on the major axes. The droplets are elongated along its major axis and flattened along the normal to the film. The orientational angle, α , and the aspect ratios of the ellipsoids, $l_b = a/b$ and $l_c = a/c$, are independent of droplet size, but they are determined, besides parameter p , by initial droplet shape, orientation, and matrix parameters. Figure 4(b) shows the dependences $\alpha(p, \alpha_0)$ and $l_b(p, \alpha_0)$ calculated for typical values of l_0 and A .

It should be noted that the validity of the model proposed is restricted by the case of a large enough initial droplet non-sphericity (say $l_0 \geq 1.1$, for evaluation) when the

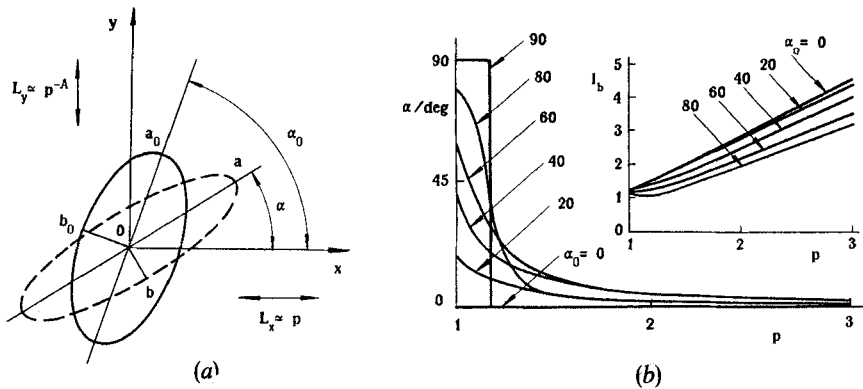


Figure 4. (a) Illustration of droplet reorientation in the plane of the PDLC film on stretching from the initial state with orientational angle, α_0 , and droplet axes, a_0 and b_0 , to the state with droplet parameters α , a , and b . (b) The dependence of droplet orientational angle, α , on the degree of film extension, p , calculated with equation (2) for different initial orientational angles, α_0 , and for $A=0.4, l_0=1.2$. The inset shows the dependence of droplet aspect ratio l_b on p for different α_0 . The numbers near the curves are the values of angle α_0 .

contribution to the free energy of the nematic inside the droplet cavity, caused by droplet shape distortion, is dominant. For the values of $l_0 \rightarrow 1$, it is expected that surface alignment effects at the droplet walls, neglected in the model, will be in competition with droplet shape anisotropy effects, and in round droplets, the surface interactions will be dominant (for more detailed discussion see, for example, [10, 11, 15]).

3.2. Description of optical parameters

To simplify the situation, we assume that: (i) monochromatic light with arbitrary polarization is incident normally to the film surface; (ii) only single scattering is supposed in the PDLC film; (iii) the interdroplet interference [16] is negligible. Because in our transmittance measurements we have used laser light, thin PDLC films with a low concentration of LC droplets, and a detector with a small acceptance angle, the assumptions made appear to be quite acceptable for our experiments. In the following consideration, we omit, for brevity, the details and adduce only the main equations used in the optical model of the stretched PDLC film.

Applying the general approach for a thin layer of independent, anisotropic, scattering objects [17], it may be shown that under the assumptions used, the intensity of light transmitted by the stretched PDLC film is described by the expression

$$I = I_{\parallel} + I_{\perp} = \frac{1}{2} [I_{\parallel 0} \exp(-\tau_{\parallel}) + I_{\perp 0} \exp(-\tau_{\perp})], \tag{3}$$

where $I_{\parallel 0}$ and $I_{\perp 0}$ are the intensities of the components of incident light polarized parallel and perpendicular to the stretch direction, respectively; τ_{\parallel} and τ_{\perp} are optical densities for the parallel and perpendicular components, which are expressed after averaging over the droplet orientations and sizes as

$$\begin{pmatrix} \tau_{\parallel} \\ \tau_{\perp} \end{pmatrix} = NL \int_0^{\infty} \frac{2}{\pi} \int_0^{\pi/2} \left[\begin{pmatrix} \sigma_1 \\ \sigma_2 \end{pmatrix} \cos^2 \alpha(\alpha_0) + \begin{pmatrix} \sigma_2 \\ \sigma_1 \end{pmatrix} \sin^2 \alpha(\alpha_0) \right] d\alpha_0 f(a_0) da_0. \tag{4}$$

Here N is the average number of LC droplets per unit volume; $L = L_0/p^B$ is the thickness of the film, where L_0 is the initial film thickness; σ_1 and σ_2 are total scattering cross

sections of a single droplet for light polarized parallel and perpendicular to major axis of the droplet, respectively; $f(a_0)$ is the droplet size distribution function; and the relation between α and α_0 is defined by equation (2).

As it is evident from equations (3) and (4), the principal transmittances of stretched PDLC film, T_{\parallel} and T_{\perp} , may be expressed as

$$T_{\parallel, \perp} = \exp(-\tau_{\parallel, \perp}). \quad (5)$$

The total scattering cross sections σ_1 and σ_2 of the supra-micron-size droplets under consideration may be found within the anisotropic modification of the anomalous diffraction approach proposed by Zumer [18]

$$\begin{pmatrix} \sigma_1 \\ \sigma_2 \end{pmatrix} = 2 \operatorname{Re} \left\{ \int_s \left[1 - \begin{pmatrix} T_{11} \\ T_{22} \end{pmatrix} \right] dS \right\}, \quad (6)$$

where T_{11} and T_{22} are diagonal elements of the Jones matrix for light passing through the droplet. The integral in equation (6) extends over the projection area of the droplet on to the plane orthogonal to the direction of the incident light. The optical anisotropy of the polymer matrix is taken into account in the calculation of T_{11} and T_{22} . In our computations of σ_1 and σ_2 , the surface integral in equation (6) was calculated numerically as a power series on parameter c/λ [19, 20], where λ is the light wavelength, for the bipolar nematic director distribution inside the droplet. The distribution was obtained by numerical minimization of the droplet free energy in one constant approximation for tangential boundary conditions at the droplet surface [21].

3.3. Mechanisms determining optical behaviour of stretched PDLC film

A close inspection of the model equations reveals that the stretching of PDLC film yields the following effects:

- (1) The orientational ordering of the droplets results in the transition from the optically isotropic state of the film when $\tau_{\parallel} = \tau_{\perp} \simeq \langle \sigma_1 + \sigma_2 \rangle / 2$ to the anisotropic state with $\tau_{\parallel} \simeq \langle \sigma_1 \rangle$ and $\tau_{\perp} \simeq \langle \sigma_2 \rangle$, where $\langle \rangle$ denotes an averaging over the droplet sizes. This process makes the main contribution to the ability of the PDLC film to polarize the incident light. The transmitted light will be partially polarized either parallel to the stretch direction (if $\sigma_1 < \sigma_2$) or perpendicular to it (if $\sigma_1 > \sigma_2$), depending on the optical parameters of the LC and polymer matrix.
- (2) In the preferred case of index match, $n_m = n_o$, where n_o is the ordinary refractive index of the LC, and simultaneous absence of matrix anisotropy, for the bipolar droplet, we always have $\sigma_1 > \sigma_2$. Stretching the film results in an increase in σ_1 and a decrease in σ_2 , because the LC molecules everywhere in the elongated droplet tend to align along the droplet major axis, thus leading to an alteration of effective refractive index matching for various components of incident light. This effect is illustrated in figure 5, where the dimensionless scattering efficiency factors of the droplet, $Q_{1,2} = \sigma_{1,2} / \sigma_g$, are shown as functions of droplet diffraction parameter, kc , and aspect ratio, l (here $\sigma_g = \pi a_0^2 p^B / l_0$ is the geometrical cross section of the droplet in the direction of the incident light which is perpendicular to the droplet major axis, and $k = 2\pi n_m / \lambda$ is the wavenumber inside the polymer matrix; for the sake of simplicity, we also assume here that the droplet is an ellipsoid of revolution). Since $\sigma_1 > \sigma_2$, the transmitted light is preferably polarized perpendicular to the stretch direction.

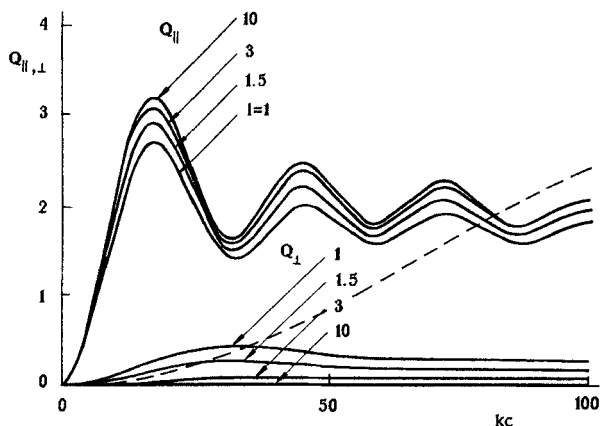


Figure 5. The dependence of dimensionless principal scattering efficiency factors of an ellipsoidal nematic droplet with bipolar configuration, $Q_{1,2} = \sigma_{1,2}/\sigma_g$ (where σ_g is the geometrical cross section of the droplet) on the diffraction parameter, kc , for the following set of refractive indices: $n_m = n_o = 1.52$, $n_e = 1.7$, and for different values of aspect ratio, l . The numbers near the curves are values of the parameter l . The broken curve corresponds to $l = 10$ and $n_m = 1.50$. Matrix anisotropy is neglected.

The data presented in figure 5 confirm that it is more effective to produce a PDLC polarizer by stretching or shearing PDLC film, as compared with the electromagnetic field accompanied matrix polymerization process [6, 7]. This is because, in the first case, σ_2 becomes much lower with stretching than that for the polymerization process, when the droplet shape is similar to a sphere ($l \approx 1$).

- (3) In the case of index mismatch, $n_m \neq n_o$, which may be caused, in particular, by increasing the matrix anisotropy on stretching (i.e. $n_m(p) \neq n_o$), the behaviour of dependence $Q(kc)$ is different from that described above. Although in this case Q_1 increases and Q_2 decreases with increasing l for fixed kc , as discussed earlier, the limiting value of Q_2 for large l is not now 0 (the limiting dependence $Q_2(kc)$ for $n_m = 1.50$ is shown by the broken curve in figure 5). For small values of kc , before the first maximum of $Q_2(kc)$, we have

$$\lim_{l \rightarrow \infty} Q_2(kc, l) \approx 2[(n_o/n_m) - 1]^2 (kc)^2 \tag{7}$$

and the upper kc -limit,

$$\lim_{kc \rightarrow \infty} Q_2(kc, l) = 2,$$

is identical to

$$\lim_{kc \rightarrow \infty} Q_1(kc, l) = 2.$$

The result is that the scattering anisotropy, $Q_1 - Q_2$, controlling the extinction ratio of the PDLC polarizer (in accordance with equations (4) and (5), $T_{\perp}/T_{\parallel} \approx \exp \langle (Q_1 - Q_2) \rangle$) decreases with increasing kc . The maximum $Q_1 - Q_2$ corresponds to the first maximum of dependence $Q_1(kc)$.

- (4) The next factor governing the optical behaviour of droplets is the lowering of the droplet thickness as $c = c_0/p^B$, which provides the changes in droplet

scattering cross sections according to the $\sigma_1(kc, l)$ and $\sigma_2(kc, l)$ dependences at a fixed value of k .

- (5) Finally, the increase in σ_1 and σ_2 caused by the growth of droplet geometrical cross section as $\sigma_g \approx p^B$ is compensated by the decrease in droplet number density per unit surface area of the film, formally expressed in equation (4) as dependence $L \approx p^{-B}$. Taking into account this simplification and introducing the volume fraction occupied by the droplets in the film, C_v , which is connected with N by equation $N = 3C_v l_0 l_1 / 4\pi \langle a_0 \rangle^3$, we can rewrite equation (4) in a more convenient form

$$\left(\begin{array}{c} \tau_{\parallel} \\ \tau_{\perp} \end{array} \right) = \frac{3}{4} C_v L_0 l_1 \frac{\left\langle a_0^2 \frac{2}{\pi} \int_0^{\pi/2} \left[\left(\frac{Q_1}{Q_2} \right) \cos^2 \alpha(\alpha_0) + \left(\frac{Q_1}{Q_2} \right) \sin^2 \alpha(\alpha_0) \right] d\alpha_0 \right\rangle}{\langle a_0^3 \rangle}. \quad (8)$$

Analysis of the mechanisms described shows that the extinction ratio of the polarizer, T_{\perp}/T_{\parallel} , reaches its maximum when all droplets are perfectly ordered along the stretch direction and the following condition is satisfied:

$$\rho \approx 4.1, \quad (9)$$

where $\rho = 2k\bar{c}[(n_e/n_m - 1)]$ is the phase shift of the \parallel -polarized component inside the droplet, $\bar{c} = \langle a_0 \rangle / p^B$ is the average droplet thickness, and n_e is the extraordinary refractive index of the LC. The condition (8), as well as the maximum of droplet scattering anisotropy, $Q_1 - Q_2$, discussed earlier, correspond to the first maximum of dependence $Q_1(kc)$.

4. Comparison with experiment and discussion

Figure 6 shows the principal extinction coefficients of the PDLC film, $W_{\parallel, \perp} = \tau_{\parallel, \perp} / C_v L_0$, as functions of parameter p . Experimental points were derived using equation (6) from averaged $T_{\parallel, \perp}(p)$ dependences measured for several PDLC films with different values of C_v and L_0 , the effect of film surface defects being eliminated. The theoretical curves were calculated from equations (2), (6) and (8) with the following set of parameters: $\lambda = 633$ nm, $A = 0.4$, $B = 0.6$, LC principal refractive indices $n_o = 1.52$, $n_e = 1.72$, and, lastly, the $n_{m\parallel, \perp}(p)$ dependences were the same as in figure 3. The droplet aspect ratios l_0 and l_1 were used as fitting parameters. To describe the droplet size distribution function $f(a_0)$, we attracted the generalized gamma-distribution [22]

$$f(a_0) = \frac{\eta(\mu/\eta)^{(\mu+1)/\eta}}{\Gamma[(\mu+1)/\eta]} \frac{a_0^\mu}{a_{0m}^{\mu+1}} \exp \left[-\frac{\mu}{\eta} \left(\frac{a_0}{a_{0m}} \right)^\eta \right], \quad (10)$$

where Γ is the gamma-function, a_{0m} is the mode of distribution, and μ and η are the distribution parameters. The model calculations were performed using the parameters: $a_0 = 0.6$ μm , $\mu = 4$, and $\eta = 0.4$, which provide a good description of our transmittance data, but differ slightly from those describing the experimental size distribution function (see experimental section). The main difference is that the fitted value of a_0 (0.6 μm) is smaller than the experimental one (≈ 1 μm). Obviously, this is a result of poor accuracy of the optical microscopy measurements, especially for the region of small droplet sizes, leading to increase in the measured values of a_0 . This conclusion is also supported by scanning electron microscopy (SEM) data presented elsewhere [12]. Therefore, our correction for the parameters of the droplet size distribution function is expected to be quite acceptable.

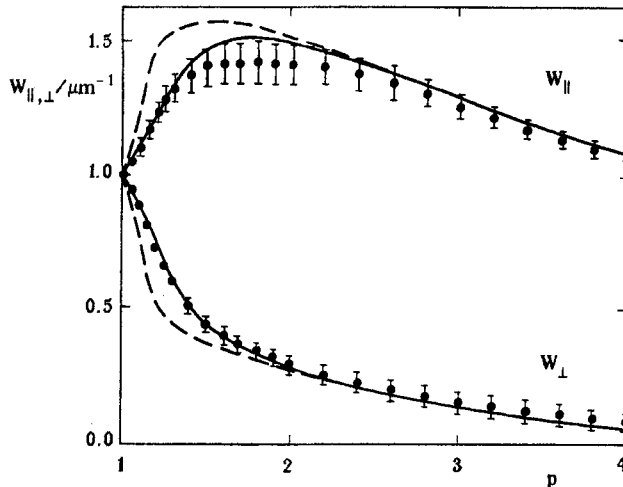


Figure 6. Extinction coefficients of stretched PDLC film, $W_{||, \perp} = \tau_{||, \perp} / C_v L_0$, as a function of the degree of film extension, p , for incident light polarized parallel ($W_{||}$) and perpendicular (W_{\perp}) to the stretch direction. The circles with bars represent the average experimental data obtained from several PDLC films with different droplet volume fractions and film thicknesses. The solid curves are model fits using the parameters: $\lambda = 633 \text{ nm}$, $A = 0.4$, $B = 0.6$, $l_0 = l_1 = 1.5$, $n_o = 1.52$, $n_e = 1.72$, $n_{m||, \perp}(p)$ presented in figure 3, and the following parameters of the size distribution function $a_{0\text{max}} = 0.6 \mu\text{m}$, $\mu = 4$ and $\eta = 0.4$. The broken curves are fits with $l_0 = 1.2$, the other parameters being the same.

The best model fit was obtained with $l_0 = l_1 = 1.5$. This value of l_1 agrees well with SEM data for PVA based PDLC films [11, 12], but l_0 is higher than the value $l \approx 1.2$ obtained from our microscopic observations. For comparison, the calculated dependences $W_{||, \perp}(p)$ for $l_0 = 1.2$ are also presented in figure 6. The observed discrepancy appears to be a result of neglecting the presence of ‘anomalous’ droplets and, probably, surface alignment effects discussed in the experimental section. Despite this fact and the various simplifications used, the model provides a good agreement between the theoretical and experimental data.

In particular, the model explains well the non-monotonic behaviour of the $T_{||}(p)$ dependence, which can be interpreted as follows. If the current average diffraction parameter of droplets in the dispersion, $k\bar{c}$, satisfies the condition $k\bar{c}(p) > k\bar{c}_{\text{max}}$, where $k\bar{c}_{\text{max}}$ corresponds to the first maximum of the $Q_1(kc, l)$ dependence (see figure 5 and equation (9)), both alteration of $Q_1(p)$ and droplet orientation result in increase in $\tau_{||}(p)$ and decrease in $T_{||}(p)$, respectively. If $k\bar{c}(p) < k\bar{c}_{\text{max}}$, the behaviour of $T_{||}(p)$ becomes more complicated, because increase in droplet ordering competes with decrease in $Q_1(k\bar{c})$. The latter factor will be dominant with increasing p , leading to the increase in $T_{||}(p)$ observed experimentally.

5. Criteria for optimization of PDLC polarizer

From the analysis of the model and from the experimental results presented in this paper, we can formulate, in conclusion, the following requirements and ways to optimize the basic performance of a PDLC polarizer based on a stretched PDLC film:

- (a) To prevent the depolarizing effect from any surface defects on the anisotropic transmittance of stretched PDLC film, the immersion coatings should be laminated on to the film surfaces.

- (b) For fixed values of droplet volume fraction, C_v , and initial film thickness, L_0 , the maximal extinction ratio of the polarizer, T_{\perp}/T_{\parallel} , may be achieved when the stretch conditions provide the perfect droplet orientation (see figure 4 (b)) and, simultaneously, the average droplet sizes and refractive indices of the LC and polymer matrix, in the required spectral region, satisfy the criterion

$$\frac{(n_e - n_m)\bar{a}_0}{p^{\beta}l_1\lambda} \approx 0.3 \quad (11)$$

This criterion follows directly from condition (9) and allows us to estimate the optimal initial droplet sizes in PDLC polarizer. For typical values $n_e - n_m = 0.2$, $l_1 = 1.5$, and $\lambda = 400-800$ nm, we have obtained $\bar{a}_{0\max} \approx (1-2)p^{\beta} \mu\text{m}$, where the value of p corresponds to a perfect droplet orientation.

- (c) To obtain a high quality polarizer, the requirement of maximal extinction ratio should be supported by simultaneous high transmittance of perpendicularly polarized component, T_{\perp} . When the droplets are perfectly oriented, we have $T_{\perp} \approx \exp(-\bar{Q}_2)$, where \bar{Q}_2 may be obtained from equation (7) in the following form:

$$\bar{Q}_2 \approx \left(\frac{(n_o - n_m)\bar{a}_0}{p^{\beta}l_1\lambda} \right)^2, \quad (12)$$

According to equation (12), the simultaneous maxima of T_{\perp} and T_{\perp}/T_{\parallel} can be easily achieved in the case of index matching, $n_m \approx n_o$ (for the case of matrix anisotropy this condition transforms into $n_m(p) \approx n_o$, where p is determined by the criterion (11)). On the other hand, the mismatch of indices results in increase in the p value required to maximize T_{\perp} so that condition (11) may be violated.

- (d) The magnitude of the switching electric field needed for the reorientation of the bipolar configurations in PDLC film normally to the film surface depends on droplet shape as $E \approx (l_c^2 - 1)^{1/2}$ [9]. Therefore, the minimization of switching voltages of an electrically controlled PDLC polarizer from polarizing to non-polarizing (clear) state, when $T_{\parallel} = T_{\perp}$, requires that the droplet aspect ratio l_c must be minimized; the requirements (b) and (c) must be satisfied. According to the model, this requirement can be fulfilled with the droplets having minimal initial shape anisotropy and smooth surfaces.

References

- [1] FERGASON, J. L., 1985, *Soc. Inf. Displays Int. Symp. Dig. Tech. Papers*, **16**, 68.
- [2] DOANE, J. W., VAZ, N. A., WU, B.-G., and ZUMER, S., 1986, *Appl. Phys. Lett.*, **48**, 269.
- [3] DRZAIĆ, P. S., 1986, *J. appl. Phys.*, **60**, 2142.
- [4] VAZ, N. A., SMITH, G. W., and MONTGOMERY, G. P., 1987, *Molec. Crystals liq. Crystals*, **146**, 1; 1987, *Ibid.*, **146**, 17.
- [5] DOANE, J. W., 1990, *Liquid Crystals: Applications and Uses*, edited by B. Bahadur (World Scientific), p. 361.
- [6] DOANE, J. W., CHIDISHIMO, G., and VAZ, N. A., 1987, USA Patent No. 4 688 900.
- [7] MARGERUM, J. D., LACKNER, A. M., RAMOS, E., LIM, K.-C., and SMITH, W. H., 1989, *Liq. Crystals*, **5**, 1477.
- [8] ZYRYANOV, V. Y., SMORGON, S. L., and SHABANOV, V. F., 1991, *Summer European Liquid Crystal Conference, Vilnius (Lithuania)*, Abstracts, p. 89.
- [9] WU, B.-G., ERDMANN, J. H., and DOANE, J. W., 1989, *Liq. Crystals*, **5**, 1453.
- [10] DRZAIĆ, P. S., 1988, *Liq. Crystals*, **3**, 1543.
- [11] DRZAIĆ, P. S., and MULLER, A., 1989, *Liq. Crystals*, **5**, 1467.
- [12] HAVENS, J. R., LEONG, D. B., and REIMER, K. B., 1990, *Molec. Crystals liq. Crystals*, **178**, 89.

- [13] ONDRIS-CRAWFORD, R., BOYKO, E. P., WAGNER, B. G., ERDMANN, J. H., ZUMER, S., and DOANE, J. W., 1991, *J. appl. Phys.*, **69**, 6380.
- [14] HOSHINO, S., DOWERS, J., LEGRAND, D. G., KAWAI, H., and STEIN, R. S., 1962, *J. polym. Sci.*, **58**, 185.
- [15] KOVAL'CHUK, A. V., KURIK, M. V., LAVRETOVICH, O. D., and SERGAN, V. V., 1988, *Zh. éksp. teor. Fiz.*, **94**, 350 (1988, *Sov. Phys. JETP*, **67**, 1069).
- [16] ZUMER, S., GOLEMME, A., and DOANE, J. W., 1989, *J. opt. Soc. Am. A*, **6**, 403.
- [17] VAN DE HULST, H. C., 1957, *Light Scattering by Small Particles* (Wiley).
- [18] ZUMER, S., 1988, *Phys. Rev. A*, **37**, 4006.
- [19] YAKOVLEV, D. A., 1991, *Optika Spektrosk.*, **71**, 788 (in Russian).
- [20] APHONIN, O. A., and YAKOVLEV, D. A., 1992, *14th International Liquid Crystal Conference*, Pisa, Abstracts, p. 944.
- [21] KRALJ, S., and ZUMER, S., 1992, *Phys. Rev. A*, **45**, 2461.
- [22] SHIFRIN, K. S., 1983, *Wvedenie v Optiku Okeana* (Gidrometeoizdat).